International Journal on Emerging Technologies **11**(3): 975-982(2020)
ISSN No. (Print): 0975-8364
ISSN No. (Online): 2249-3255

Restoration of Compressed Image using Hard Thresholding Method

M.S. Sujithra[1] and N. Sugitha[2]
[1]Research Scholar, Department of CSE,
Noorul Islam Centre for Higher Education, Kumaracoil (Tamilnadu), India.
[2]Associate Professor, Department of Department of IT,
Noorul Islam Centre for Higher Education Kumaracoil, (Tamilnadu), India.

(Corresponding author: M.S. Sujithra)
(Received 16 March 2020, Revised 15 May 2020, Accepted 18 May 2020)
(Published by Research Trend, Website: www.researchtrend.net)

ABSTRACT: In recent years, the major problem faced by the image compression is blocking artifacts which are due to high compression rates and lack of quantization bit constraints. One of the methods is deblocking which is used for restoring the compressed image. The deblocking method is broadly classified asafiltering approach and restoration of transform coefficients. The existing methods either use filters or approximate the DCT coefficients to remove the blocky edges. The proposed method uses a hard thresholding method to remove blocking artifacts. The threshold value is derived from the degraded image. The hard thresholding method includes the following steps: Forward transform, Thresholding, and Inverse transform. Even though the decomposition of the transform is different, this paper considers the transform like Wavelet Transform, Contourlet Transform, Curvelet Transform, and Shearlet Transform using a hard thresholding method. The level of decomposition of the transform is represented as N=4. The restored images are also analyzed based on the based on both Objective and Subjective fidelity measuresand the results are also compared with existing methods based on the performance metrics like PSNR, SSIM, EPI, FSIM.

Keywords: Artifacts, Contourlet, Curvelet, Shearlet, thresholding, Wavelet.

Abbreviations: JPEG, Joint Photographic Experts Group; BDCT, Block-based Discrete Cosine Transform; MAP, Maximum of a-Posteriori; POCS,Projection Onto Convex Sets;

I. INTRODUCTION

A wide range of fascinating applications of digital images includes medical images, satellite images, and in areas like astronomy, Research, and Technology. The significant aspect of the imaging is to reduce the size of the image without comprising the quality of the image. The two reasons for reducing the size of the image is: to maintain less storage space and to increase the transmission speed. The JPEG and JPEG 2000 [1] are the traditional standard which reduces image size. The JPEG standard for lossy compression has three sub-stages which include Block-based Discrete Cosine Transform (BDCT), quantization, and Huffman encoding. The fundamental issue of image compression is that it misfortunes vital information. These inevitable losses of information are created due to quantization- bit constraints that create blocky structure called blocking artifacts. The visual imperfections that the artifacts caused are due to block bands created by degrading the original edges or degrading the corner points of the blocks.

Ramteke *et al.,* [2] described the various blind deconvolution techniques used for image restoration. George *et al.,* [3] classified the existing JPEG restoration techniques in the spatial domain into three different categories: filtering method, estimation theoretic methods, and projection onto convex sets methods. Additionally, by considering the frequency domain aspects, the existing restoration of the compressed image in the literature is categorized as deblocking methods and estimation/learning-based methods.

The deblocking methods used for restoring the compressed images are classified as filtering approach and restoration of DCT coefficients. Based on removing artifacts in compressed images, the filters are classified based on the domain: spatial filters and frequency filters. The spatial filters, which manipulates the image plane directly with the help of the convolution kernels is applied directly on the compressed image [4-11].

The frequency-domain filters [12-20], neglects the presence of interference in the image, which deals with transform coefficients within the image and the restoration is on the footing of the frequency response of correction filter, which was set up for the inverse of the frequency domain.

The Restoration of Transform Coefficients [21-28] reconstructs the image transform coefficients directly. The image transforms coefficients after quantization of compressed image is taken into consideration which has one DC coefficient and 63 AC coefficients.

The Estimation / learning methods include Maximum of a-Posteriori; MAP [29-33], Projection Onto Convex Sets; POCS [34-39] and Sparse dictionary learning [40-48]. Additionally the various other methods [49-54] are also used to remove artifacts. The existing methods restore the compressed image without any knowledge of degradation whereas the proposed method derives the threshold value from the compressed image and tries to remove the blocking artifacts.

The proposed method restores the compressed image using a Hard thresholding method and this method considers the transforms like Wavelet, Curvelet, Contourlet, and Shearlet Transform to remove blocking artifacts.

The paper is organized as Section II describes the decomposition of various transform and Section III describes the proposed method for Restoration of the compressed image using hard thresholding method, Section IV describes the experimental results and comparison between existing methods and Section V concludes the paper.

II. DECOMPOSITION OF TRANSFORM

The multi-scale of decomposition is of Wavelet Transform, Curvelet Transform, Contourlet Transform, and Shearlet Transform is as follows.

A. Multi-scale decomposition of Wavelet Transform
The two-dimensional Discrete Wavelet Transform [55] decomposes the image, into four components which maintain the temporal and spatial information. The decomposition of the wavelet divides the compressed image into four components: LL, LH, HL, and HH. The LL represents the low-resolution components called approximations and LH, HL and HH represent the horizontal, vertical, and diagonal components called detailed coefficients. The multi-level decomposition of the wavelet is represented in the Fig. 1.

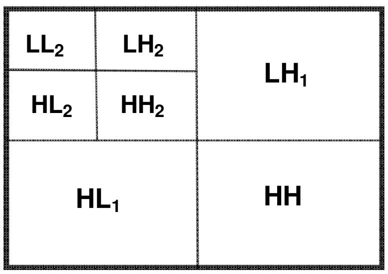

Fig. 1. Decomposition of Wavelet Transform.

The forward transform of Discrete Wavelet Transform is calculated from the image by passing through a set of filters H and G, where H and G represent the low pass filter and the high pass filter respectively. The approximations coefficients are derived from low pass filter and detailed coefficients are derived from high pass filter respectively. The two filters perform downsampling by 2 and treat half of the sub-bands of H and G filters respectively the filter is termed as quadrature mirror filter.

B. Multi-scale decomposition of Curvelet Transform
The Curvelet Transform [56] is also a multiscale transform but it is highly anisotropic and has high directional sensitivity compared to Wavelet Transform.
The Curvelet Transform based image decomposition has four steps: subband decomposition, smooth partitioning, renormalization and analysis of ridgelet. The basic decomposition of Curvelet Transform is illustrated in Fig. 2. Let P be the image, then Δ_1, Δ_2, and P_3 represent the subband created using additive wavelet transform. The Ridgelet Transform is then performed on the subbands Δ_1, Δ_2. Based on the different frequency components of the image, the subband decomposition of the Curvelet Transform divides the image into different sub-bands. But it doesn't outperform the down sampling as Wavelet Transform.
The image P is decomposed in f objects is represented using the equation is

$$f \rightarrow (P_0 f, \Delta_1 f, \Delta_2 f) \quad (1)$$

Where $\Delta_1 = P_{i-1} - P_i$ is the difference between the two consecutive wavelet plane. The smooth partitioning is done by applying windowing function $W_Q(x_1, x_2)$ across each sub band and is given by $\Delta_s f \rightarrow (W_Q \Delta_s f)_{Q \in Q_S}$.

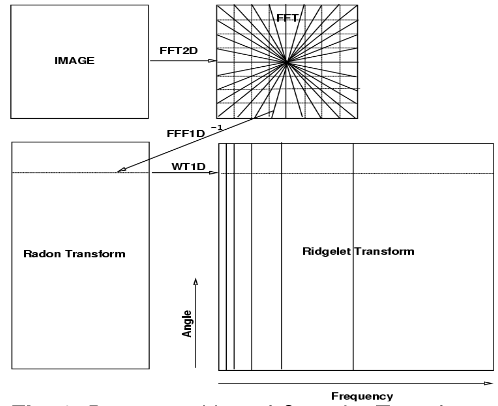

Fig. 2. Decomposition of Curvelet Transform.

Each dyadic square is renormalized to unit scale and then perform a discrete ridgelet transform of each square. The Curvelet Transform represents the lines and edges in an image efficiently.

C. Multi-scale decomposition of Contourlet Transform
The Contourlet Transform [57-58] has the potential to handle the 2D singularities like edges, lines effectively. The Contourlet Transform represents the images in various dimensions like multi-scale, multi-direction, and multi-resolution. The Contourlet Transform decomposition is illustrated in Fig. 3. To represent the images in different resolution the Laplacian pyramid is used and for representing the image in different directional natures, the Directional Filter Bank (DFB) is used. At each level, the Laplacian pyramid decomposes the image into two versions: low pass image: LL and band-pass images: LH, HL, HH. Downsampling the original image to produce the low pass image and the remaining sub-bands called band-pass images. The Directional Filter Bank takes the band-pass inputs as input and produces the contourlet coefficients as output.

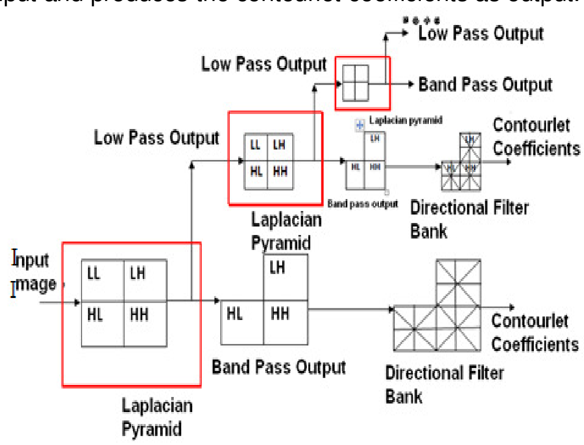

Fig. 3. Decomposition of Contourlet Transform.

D. Multi-scale decomposition of Shearlet Transform
Shearlet Transform [59] optimally represents the 2D singularities of the image like edges, lines effectively. The Shearlet Transform signifies the image in different

dimensions like multi-scale and multi-directional geometry of the image. The decomposition of Shearlet Transform is illustrated in Fig.4.

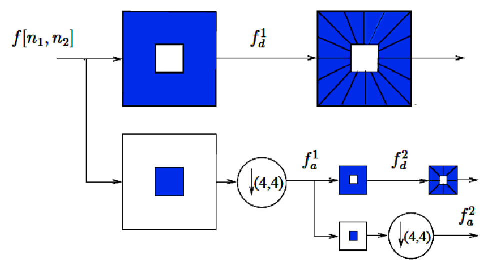

Fig. 4. Decomposition of Shearlet Transform.

In Shearlet Transform, at each level of decomposition, the image is split into four levels and generates sub-band images. The two-dimensional basis function of the Shearlet Transform is given as

$$A_{DS}(\psi) = \{\, \psi_{j,k,l}(x) = |\det(B)|^{\frac{j}{2}}\, \psi(S^l D^l x - l) : j \, \varepsilon\, \mathbb{Z}, k : l\, \varepsilon \mathbb{Z}^2 \qquad (2)$$

Where, $\psi\ \varepsilon\ L^2\ (\mathbb{R}^2)$ and D, S are the invertible 2x2 matrices. The dilation matrix and shearing matrix are represented using D^l and S^l respectively. The Shearlet Transform represented in equation 2 performs translation, scaling, and also represent various orientation using shearing. The Shearlet basis function of an image is represented using F and is given as, F = { $\psi_{j,k,l}$ (x):j ,l ε $\mathbb{Z}$, k ε $\mathbb{Z}^2$ }, then the approximation function, F_N is given as

$$F_N = \langle F, \psi_{j,k,l} \rangle \psi_{j,k,l} \qquad (3)$$

The N_{term} approximation error ε_N is obtained by approximating the set of basis functions derived from the image.

$$\varepsilon_N = \| F - F_N \| = \sum |\langle F, \psi_{j,k,l} \rangle|^2 \qquad (4)$$

representation and also efficiently captures the intrinsic The N-term approximation which is derived from the set of the basis function is minimized to obtain the image closed to the original image.

Even though lots of transforms are evolved after Discrete Cosine Transform the JPEG compression which uses Discrete Cosine Transform plays a vital role in image compression and produces the blocking artifacts. With the help of transform like Discrete Wavelet Transform, Curvelet, Contourlet, and shearlet transform, the proposed method tries to restore the compressed image.

III. PROPOSED METHOD

The hard thresholding method which is used for removing artifacts in the compressed image has three steps: Forward Transform, thresholding, and Inverse Transform. The restoration of the compressed image is illustrated in Fig. 5 which fed the compressed image as input and produces the restored image as output. The sqtwolog [60] is the universal thresholding method is used for calculating the threshold value from the variance of HH sub-bands. The threshold λ is determined as

$$\lambda = \boldsymbol{\sigma}\sqrt{2 \log n} \qquad (5)$$

Where n is the level of decomposition and

$$\sigma = \frac{median(|w|)}{0.6745} \qquad (6)$$

Where w refers to the coefficients of HH sub-bands.

The transform domain restoration is based on the thresholding of the signal. The thresholding is of two types: hard thresholding and soft thresholding. The hard thresholding is expressed as:

$$T_{hard}(d_{j,k}) = \begin{cases} d_{j,k}, & if\ |d_{j,k}| \geq \lambda \\ 0, & if\ |d_{j,k}| < \lambda \end{cases} \qquad (7)$$

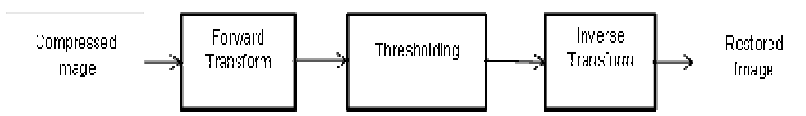

Fig. 5. Restoration of the compressed image using Hard Thresholding Method.

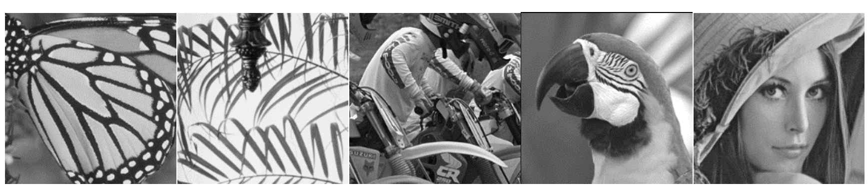

Fig. 6. Five Test Images.

The hard thresholding method is used to remove blocking artifacts since the coefficients greater than the threshold level is not affected. The hard thresholding algorithm is described as follows.

1. The compressed image is decomposed into multiple frequency levels and the error/noise variance is estimated from the decomposed high-frequency coefficients.
2. Each level uses Directional Filter Bank (DFB) procedure to decompose the high-frequency coefficients into several directional sub-bands (horizontal, vertical, and diagonal) and the threshold value is estimated from the computed noise variance of the sub-bands.
3. The hard threshold value is applied to all transform coefficients of the sub-bands for removing blocking artifacts. The transform coefficients greater than the threshold is left unchanged and the remaining transform coefficients are suppressed.
4. The resultant output image is obtained by applying an inverse transform on the transform coefficients.

The level of the decomposition is usually represented as N and even though different transforms like Wavelet, Contourlet, Curvelet, and Shearlet Transform are used in the Hard thresholding method the value of N= 4 is considered.

IV. EXPERIMENTAL RESULTS

The experimental results obtained analyze the performance of restored images.

The results of the proposed method are compared with existing methods which are based on transform coefficients. Five widely used test images of size 256 x 256 gray-scales are considered for the comparative study.

The performance metrics considered to compare the restoration of JPEG compressed images are PSNR, SSIM [61], UIQI [62], FSIM [63], and EPI.

The Peak Signal to Noise Ratio (PSNR) is calculated as

$$PSNR = 10\, log_{10}\left(\frac{255^2}{MSE}\right) \tag{8}$$

Where, MSE represents squared error between two images, and M and N be the number of rows and columns in the image respectively.

$$MSE = \sum_{M,N} \frac{[I_1(m,n) - I_2(m,n)]^2}{M*N} \tag{9}$$

Where, $I_1(m,n)$ be the original image and $I_2(m,n)$ represents the restored image.

The Structural Similarity Index (SSIM) measures the image quality based on the similar features. The index value lies between -1 to 1. The SSIM calculation is given as

$$SSIM(x,y) = \frac{2(\mu_x+\mu_y+C_1)(2\sigma_{xy}+C_2)}{(\mu_x^2+\mu_y^2+C_2)(\sigma_x^2+\sigma_y^2+C_2)} \tag{10}$$

Where μ_x and μ_y represent the mean of x and y respectively as well as σ_x^2 and σ_y^2 be the variance of x and y respectively. The σ_{xy} represents the covariance of xy and C_1 and C_2 are the constants used for denominator stabilization.

The Universal Image Quality Index (UIQI) measures the distortions of the image and the value lie in-between -1 to 1 and it is defined as

$$Q = \frac{4\sigma_{xy}\bar{x}\bar{y}}{(\sigma_x^2+\sigma_y^2)[\bar{x}^2+\bar{y}^2]} \tag{11}$$

Where $\bar{x}$ and $\bar{y}$ represent the mean of x and y respectively.

The Feature Similarity index (FSIM) measures the quality of the image based on Phase Congruency maps (PC) and Gradient Magnitude (GM) maps derived from the original image f_1 and reconstructed image f_2. The FSIM is given as

$$FSIM = \frac{\sum_{x\epsilon\Omega} S_L(x) PC_m(x)}{\sum_{x\epsilon\Omega} PC_m(x)} \tag{12}$$

$$S_L(x) = S_{PC}(x).S_G(x) \tag{13}$$

$$S_{PC}(x) = \frac{2PC_1(x).PC_2(x)+T_1}{PC_1^2+PC_2^2+T_1} \tag{14}$$

$$S_G(x) = \frac{2G_1(x).G_2(x)+T_2}{G_1^2+G_2^2+T_2} \tag{15}$$

Where, T_1, T_2 represents constant, PC_1, PC_2, G_1, G_2 be the PC maps and GM maps extracted from f_1 and f_2 respectively.

The Edge Preserving Index (EPI) is computed between the original image and restored image is given as

$$EPI = \frac{\sum_{i=1}^{M}\sum_{j=1}^{N-1}|y(i,j+1)-y(i,j)|}{\sum_{i=1}^{M}\sum_{j=1}^{N-1}|x(i,j+1)-x(i,j)|} \tag{16}$$

Where x be the original image and y be the restored image.

Table 1 represents the comparison of the proposed method with the existing method based on PSNR value and also it is differentiated based on the transforms used in the hard thresholding method. The quality factor, QF of the compressed images is 10.

Table 1: Comparison of the proposed method with the restoration of transform coefficients methods.

Images	Existing Method						Proposed Method			
	JPEG	[25]	[24]	[26]	[28]	[27]	Wavelet	Curvelet	Contourlet	Shearlet
Butterfly	25.23	23.77	25.71	25.21	25.66	25.03	25.08	25.23	23.63	**25.73**
Lena	27.71	27.35	28.25	27.55	28.22	28.43	28.58	28.68	27.13	**29.15**
Parrot	28.94	28.63	29.32	28.97	29.53	29.58	28.85	28.91	26.99	**29.6**
Bike	24.06	23.77	24.28	24.01	24.25	**24.43**	24.04	24.09	22.38	24.33

Table 2 represents the comparison of the proposed method with the existing dictionary learning methods based on PSNR value and also it is differentiated based on the transforms used in the hard thresholding method. The quality factor, QF of the compressed images is 5.

Table 3 represents the comparison of the proposed method with uses Transform like Wavelet, Contourlet Curvelet, and Shearlet Transform in Hard Thresholding algorithm. The comparison is represented for the images with the quality factor QF= 5,10.

The Objective fidelity performance metrics are indicated in Table 1 and 2. For the Subjective fidelity performance, the following images represent the compressed image, hard thresholding method based on Transforms like Wavelet, Contourlet Curvelet, and Shearlet Transform. The comparison is represented for the images with the quality factor QF= 10. From the Objective and Subjective performance metrics, it is clear that our proposed method yields better results compared to all the existing methods.

Table 2: Comparison of the proposed method with the existing dictionary learning methods.

Images	**Existing Method**			**Proposed Method**			
	JPEG	**KSVD**	**DICTV**	**Wavelet**	**Curvelet**	**Contourlet**	**Shearlet**
Butterfly	22.57	**23.8**	23.54	22.59	22.58	22.13	**23.8**
Leaves	22.48	23.66	23.27	22.49	22.52	21.9	**23.71**
Bike	21.7	22.56	22.28	21.73	21.71	21.25	**22.6**

Table 3: Comparison of the proposed method with different performance metrics.

Images	Performance metrics	QF	Compressed	Proposed Method			
				Wavelet	Curvelet	Contourlet	Shearlet
Butterfly	PSNR	5	22.57	22.59	22.58	22.13	**23.8**
	SSIM		0.7373	0.7268	0.7374	0.68	**0.8055**
	UIQI		0.9977	0.9976	0.9977	0.997	**0.9979**
	FSIM		0.7555	0.762	0.7557	0.7369	**0.8095**
	EPI		0.4699	0.4764	0.47	0.4619	**0.6004**
	PSNR	10	25.23	25.08	25.23	23.63	**25.73**
	SSIM		0.8232	0.8059	0.8247	0.769	**0.8641**
	UIQI		**0.9933**	0.9992	**0.9993**	0.9987	**0.9993**
	FSIM		0.8118	0.8105	0.8122	0.7848	**0.8585**
	EPI		0.6163	0.6058	0.6172	0.5198	**0.6873**
Leaves	PSNR	5	22.48	22.49	22.52	21.9	**23.71**
	SSIM		0.7789	0.7673	0.781	0.7277	**0.8321**
	UIQI		**0.9984**	0.9983	**0.9984**	0.9979	0.9983
	FSIM		0.7813	0.7789	0.7826	0.7591	**0.8247**
	EPI		0.6202	0.6301	0.6201	0.6373	**0.7409**
	PSNR	10	25.38	25.08	25.41	23.14	**26.06**
	SSIM		0.8618	0.8406	0.8643	0.7662	**0.8942**
	UIQI		**0.9996**	0.9994	**0.9996**	0.9991	0.9994
	FSIM		0.8413	0.8337	0.8434	0.7892	**0.8789**
	EPI		0.7314	0.719	0.7338	0.6785	**0.8053**
Parrots	PSNR	5	26.18	26.23	26.21	25.84	**27.58**
	SSIM		0.7626	0.761	0.7629	0.7353	**0.8322**
	UIQI		0.9976	0.9974	0.9976	0.9973	**0.9979**
	FSIM		0.8268	0.8593	0.8272	0.8623	**0.8861**
	EPI		0.6553	0.6779	0.6564	0.6649	**0.7569**
	PSNR	10	28.94	28.85	28.91	26.99	**29.6**
	SSIM		0.8365	0.8325	0.8367	0.7608	**0.8666**
	UIQI		**0.9994**	0.9993	**0.9994**	0.9987	**0.9994**
	FSIM		0.8961	**0.9087**	0.8962	0.879	0.9082
	EPI		0.746	0.7492	0.7474	0.7011	**0.7978**
Bike	PSNR	5	21.7	21.73	21.71	21.25	**22.6**
	SSIM		0.6575	0.6528	0.6578	0.587	**0.6895**
	UIQI		0.9953	0.9952	0.9952	0.9939	**0.9954**
	FSIM		0.7909	0.8051	0.7914	0.786	**0.8113**
	EPI		0.4628	0.4693	0.4637	0.427	**0.5623**
	PSNR	10	24.06	24.04	24.09	22.38	**24.33**
	SSIM		0.776	0.7691	**0.7776**	0.6575	0.7706
	UIQI		**0.9984**	0.998	0.9983	0.9965	0.9978
	FSIM		0.862	0.8618	**0.8629**	0.813	0.8517
	EPI		0.6067	0.6019	0.609	0.5025	**0.6597**
Lena	PSNR	5	25.85	25.88	25.85	25.88	**27.28**
	SSIM		0.6876	0.6848	0.6876	0.6639	**0.749**
	UIQI		0.9971	0.9968	0.9971	0.9968	**0.9976**
	FSIM		0.8035	0.8363	0.8034	0.8447	**0.8489**
	EPI		0.5714	0.6037	0.573	0.6433	**0.7204**
	PSNR	10	27.71	28.58	28.68	27.13	**29.15**
	SSIM		0.7895	0.7824	0.7899	0.7098	**0.7968**
	UIQI		**0.9992**	0.9991	**0.9992**	0.9985	**0.9992**
	FSIM		0.8837	**0.8913**	0.8835	0.8647	0.8807
	EPI		0.6704	0.6803	0.6723	0.6668	**0.7591**

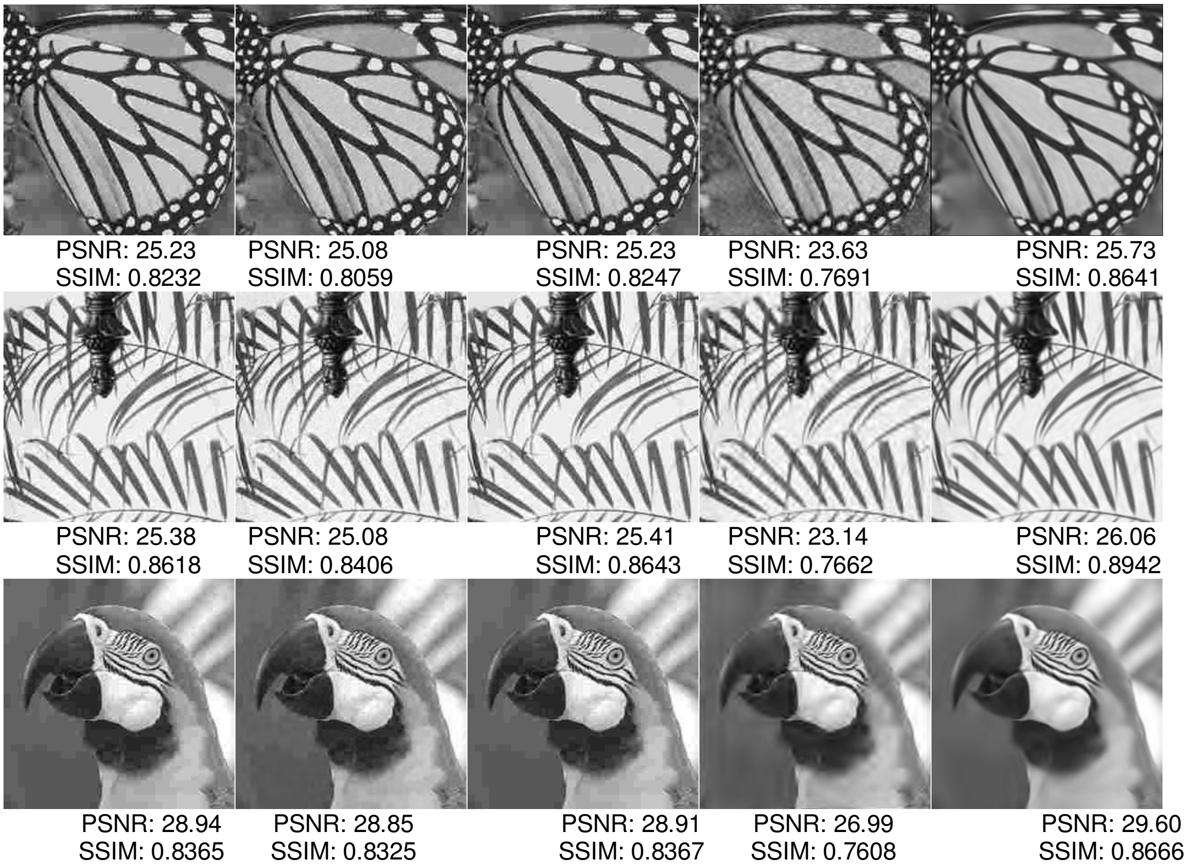

Fig. 7. a) Compressed image b) Hard thresholding method based on Wavelet Transform, c) Hard thresholding method based on Curvelet Transform, d) Hard thresholding method based on Contourlet Transform e) Hard thresholding method based on Shearlet Transform. (b,c,d,e represents proposed method)

V. CONCLUSION

This method concentrates mainly on JPEG compressed image, which uses a Discrete Cosine Transform that supports strong energy compaction. The hard thresholding method used for restoring the transform coefficients is based on a theoretical approach which tries to calculate the quantized transform coefficients. The first step and last step of hard thresholding method depend on the transform, this paper considers the different transforms like Wavelet, Contourlet, Curvelet, and Shearlet Transform. From the objective and subjective analysis, it is evident that for restoring the compressed image, the hard thresholding method based on Shearlet Transform produces state-of-art results. Specifically, the proposed method is compared with the existing restoration of transform coefficients methods and also this method removes artifacts in the image and achieves better results at a high computational cost.

VI. FUTURE SCOPE

In the future, this method is applied to various other applications like image inpainting and image classification.

Conflict of Interest. No.

REFERENCES

[1]. Heema Sharma., Shrish Dixit., Babita Pathik., and Shiv, K. Sahu. (2017). Image Compression using Wavelet transform. *International Journal of Electrical, Electronics and Computer Engineering*, *6*(1): 139-144.

[2]. Ramteke Mamta, G., and Maitreyee Dutta (2019). Review of Bling Deconvolution Technique for Image restoration. *International Journal on Emerging Technologies*, *10*(2): 334-334.

[3].. George, A.T., Dimitrios Tzovaras., and Michael Gerassimos, (2002). Blocking Artifacts detection and reduction in compressed data. *IEEE Transactions on Circuits and Systems for Video Technology*, *12*(10): 877 – 890.

[4]. Hsu, Y .F., and Chen, Y.C., (1993). A new adaptive median filter for removing blocking effects. *IEEE Transactions Consumer Electronics*, *39*(3): 510 – 513.

[5]. Jarske, T., Haavisto, P., and Defe'e, I., (1994). Post-filtering methods for reducing blocking effects from coded images. *IEEE Transactions Consumer Electronics*, *40*(3): 521–526.

[6]. Kuo, C.J., and Hseih, R.J., (1995) Adaptive post-processor for block encoded images. *IEEE Transactions on Circuits and Systems for Video Technology*, Vol. 5(4): 298–304.

[7]. Lee, Y.L., Kim, H.C., and Park, H.W., (1998). Blocking effect reduction by JPEG images by Signal Adaptive filtering. *IEEE Transactions on Image Processing*, *7*(2): 229–234.
[8]. Buyue Zhang., Jan P Allebach., (2008). Adaptive Bilateral Filter for Sharpness Enhancement and Noise Removal. *IEEE Transactions on Image Processing*, *17*(17): 664–678.
[9]. Nath, N.K., Hazarika, D., and Mahanta, A., (2010). Blocking Artifacts reduction using adaptive bilateral filtering. *Proceedings of the IEEE International Conference on Signal Processing and Communication*, pp. 1-5.
[10]. Dung, T. Vo., Truong Q Nyuyen., Sehoon Yea., and Vetro, A., (2009). Adaptive Fuzzy Filtering for Artifact Reduction in Compressed Images and Videos.*IEEE Transactions on Image Processing*, *18*(6): 1166 – 1178.
[11]. Wang, C., Zhou, J., and Liu, S., (2013). Adaptive non-local means filter for image deblocking. *Signal Processing: Image Communication*, *28*, 522–530.
[12]. Tao Chen., Hong Ren Wu., and Bin Qiu., (2002). Adaptive post filtering of Transform Coefficients for the reduction of blocking artifacts. *IEEE Transaction on Circuits Systems and Video Technology*, *11*(5): 594–602.
[13]. Luo, Y., and Ward, R.K., (2003). Removing the blocking artifacts of block based DCT compressed images. *IEEE Transaction on Image Processing*, *12*(7): 838 – 842.
[14]. Popovici, I., and Douglas, W., (2007). Locating edges and removing ringing artifacts in JPEG images by frequency-domain analysis. *IEEE Transactions on Image Processing*, *16*(5): 1470–1474.
[15]. Kim, S.D., Kim, H.M., and Ra, J.B., (1999). A deblocking filter with two separate modes in block-based video coding. *IEEE Transactions on Circuits and Systems for Video Technology*, *9*(1): 156-160.
[16]. Joch, L.P., Lainema, A., Bjntegaard, J., and Karczewicz, G., (2003). Adaptive deblocking filter. *IEEE Transactions on Circuits and Systems for Video Technology*, *13*(7): 614–619.
[17]. Tai, S., Chen, Y.Y., and Sheu, S.F., (2005). Deblocking filter for low bit rate MPEG4 video. *transactions on circuits and systems for video technology*, *15*(6): 731–733.
[18]. Averbuch, A.Z., Schclar, A., and Donoho, D.L., (2005). Deblocking of block-transform compressed images using weighted sums of symmetrically aligned pixels. *IEEE Transactions on Image Processing*, *14*(2): 200–212.
[19]. Taehwan Lim., Jiman Ryu., and Jongho Kim., (2008). Adaptive deblocking method using a transform table of different dimension DCT. *IEEE Transactions on Consumer Electronics*, *54*(4): 1–5.
[20]. Ramakrishna Palaparthi, and Vinay Kumar Srivastava, (2012). A simple deblocking method for the reduction of blocking artifacts. *IEEE Students Conference on Electrical, Electronics and Computer Science*, pp.1–4.
[21]. Minami, S., and Zakhor (1995). An optimization approach for removing blocking effects in transform coding. *IEEE Transactions on Circuits and Systems for Video Technology*, *5*(2): 74–85.
[22]. Jeon, B., and Jeong, J., (1998). Blocking artifacts reduction in image compression with block boundary dis-*IEEE Transaction on Circuits Systems and Video Technology*, *8*(3): 345–357.
[23]. Zeng, B., (1999). Reduction of blocking effect in DCT-coded images using zero-masking techniques.*Signal Processing*, *79*(2): 205–211.
[24]. Al-Fohoum. A.S., and Reza. A.M. (2001). Combined edge crispiness and statistical differencing for deblocking JPEG compressed images.*IEEE Transaction on Image Processing*, *10*(9): 1288-1298.
[25]. Shizhong Liu., and Bovil, A.C., (2002). Efficient DCT-domain blind measurement and Reduction of blocking Artifacts. *IEEE Transaction on Circuits Systems and Video Technology*, *12*(12): 1139–1149.
[26]. Lee. K., Kim. D.S., and Kim, T., (2005). Regression-based prediction for blocking artifact reduction in jpeg-compressed images. *IEEE Transaction Image Processing*, *14*(1): 36-49.
[27]. Zhai, G., Zhang, W., Yang, X., Lin, W., and Xu, Y.,(2008). Efficient Deblocking With Coefficient Regularization, Shape-Adaptive Filtering, and Quantization Constraint. *IEEE Transaction on Multimedia, 10*(5): 735-745.
[28]. Zhai, G., Zhang, W., Yang, X., Lin, W., and Xu. Y(2008). Efficient Image Deblocking Based on Postfiltering in Shifted Windows. *IEEE Transaction Circuits and Systems for Video Technology*, *18*(1): 122-126.
[29]. M.A.T. Figueiredo., and Nowak, R.D., (2003). An EM algorithm for wavelet-based image restoration. *IEEE Transactions on Image Processing*, *12*(8): 906–916.
[30]. Rourke, T.P.O., and Stevenson, R.L., (1995). Improved image decompression for reduced transform coding artifacts. *IEEE Transactions on Circuits and Systems for Video Technology*, *5*(6): 490–499.
[31]. Ozcelik Taner., Brailean, J.C., and Katsaggelos, A.K., (1995). Image and video compression algorithms based on recovery techniques using mean field annealing. *Proceedings of the IEEE*, *83*(2): 304–316.
[32]. Meier, T., Ngan, K.N., and Crebbin, G. (1999). Reduction of blocking artifacts in image and video coding. *IEEE Transactions on Circuits and Systems for Video Technology*, *9*(3): 490–500.
[33]. Xinfeng Zhang., Ruiqin Xiong., Xiaopeng Fan., Siwei Ma., and Wen Gao., (2013). Compression Artifact Reduction by Overlapped-Block Transform coefficient Estimation With Block Similarity. *IEEE Transactions on Image Processing*, *22*(12): 4613 – 4626.
[34]. Unal, G.B., and Cetin, A.E. (2001). Restoration of error-diffused images using projection onto convex sets. *IEEE Transactions on Image Processing*, *10*(12): 1836 – 1841.
[35]. Zakhor, A., (1992). Iterative procedures for reduction of blocking effects in transform image coding. *IEEE Transactions on Circuits and Systems for Video Technology*, *2*(1): 91–95.
[36]. Zou, J.J., and Yan, H., (2005). A deblocking method for BDCT compressed images based on adaptive projections”, *IEEE Transaction on Circuits and system for Video Technology*, *15*(3): 430 – 435.
[37]. Yang, Y., and Galatsanos, N.P., (1997). Removal of Compression Artifacts Using Projections onto Convex Sets and Line Process Modeling *IEEE Transactions on Image Processing*, *6*(10): 1345 -1357.

[38]. Yoon Kim., Chun-Su Park., and Sung-JeaKo., (2003). Fast POCS based post-processing technique for HDTV.*IEEE Transaction in Consumer Electronics*, *49*(4): 1438–1447.
[39]. Paek, H., and Haseyama, R.C.H., (2011). Missing intensity interpolation using a kernel PCA-based POCS algorithm and its applications", *IEEE Transactions on Image Processing*, *20*(2): 417–432.
[40]. Zheng Zhang., Jian Yang., and David Zhang., (2015). A Survey of sparse representation: algorithms and applications. *IEEE Biometrics Compendium*, *3*(1): 490–530.
[41]. Hyvarinen, A., (1999). Fast and robust fixed-point algorithms for independent component analysis. *IEEE Transactions on Neural Networks*, *10*(3): 626–634.
42]. Aharon Michal., Michael Elad., and Alfred Bruckstein., (2006). K-SVD: An algorithm for designing overcomplete dictionaries for sparse representation. *IEEE Transactions on Signal Processing*, *54*(11): 4311-4322.
[43]. Inchang Choi., and Sunyeong Kim., (2013). A learning-based Approach to reduce JPEG Artifacts in Image Matting.*Proceedings of the IEEE Conferences in Computer Vision*, Sydney, NSW, Australia, 2880–2887.
[44]. Liu, X., Wu, X., Zhou, J., and Zhao, D., (2013). Sparsity-based decoding of compressed images in Transform Domain. *Proceedings of the IEEE International Conference on Image Processing*, Melbourne, VIC, Australia, 563–566.
[45]. Chang Huibin., Michael, K., and Zeng Tieyong, (2014). Reducing Artifact in JPEG Decompression via a Learned Dictionary. *IEEE Transactions on Image Processing*, *62*(3): 718–728.
[46]. Liu, X., Wu, X., Zhou, J., and Zhao, D., (2015). Inter-block consistent soft decoding of jpeg images with sparsity and graph-signal smoothness priors. *Proceedings of the IEEE International Conference on Image Processing,* Quebeu City, QC, Canada, 1628–1632.
[47]. Liu, X., Wu, X., Zhou, J., and Zhao, D., (2016). Data-Driven Soft Decoding of Compressed Images in Dual Transform-Pixel Domain", *IEEE Transactions on Image Processing*, *25*(4): 1649-1659.
[48]. Sujithra, M.S., and Sugitha, N., (2019). Sparse Coding Strategies and Sparse Dictionary Learning. *Journal of Advanced Dynamical & Control Systems*, *11*(7): 1407-1413.
[49]. Kaushik, M.K., Chandrakala, G.C., and Raj Abhinay, (2018). Ringing and Blur Artifact Removal in Image Processing Applications. *Second International Conference on Intelligent Computing and Control Systems*, June 14-15, Madurai, India, 260-264.
[50]. Honggang Chen., Xiaohai He., Cheolhong, A., and Truong Q Nyugen., (2019). Deep Wide-Activated Residual Network-Based Joint Blocking and Color Bleeding Artifacts Reduction for 4: 2:0 JPEG-Compressed Images. *IEEE Signal Processing Letters*, *26*(1): 79-83.
[51]. Chen Zhao., Jian Zhang., Siwei Ma., Xiaopeng Fan., Yongbing Zhang., and Wen Gao. (2017). Reducing Image Compression Artifacts by Structural Sparse Representation and Quantization Constraint Prior. *IEEE Transactions on Circuits and Systems for video Technology*, *27*(10): 1-14.
[52]. Ekta Patel., and Mohit Gangwar, (2018). Analysis of novel de-blocking method for blocking artifacts reduction. *International Conference on Communication and Signal Processing*, Chennai, India, 1452-1456.
[53]. Amanjot Singh., and Jagroop Singh., (2019). Blocking Artifacts Removal of DCT based Highly Compressed Images. *Second International Conference on Intelligent Computing, Instrumentation and Control Technologies*, Kannur, Kerala.
[54]. Vincent Itier., Florentin Kucharczak., Olivier Strauss., and William Puech., (2018). Interval-valued JPEG decompression for artifact suppression. *Eighth International Conference on Image Processing Theory, Tools and Applications*, November 7-10, China.
[55]. Salesnick, I.W., (2006). A Higher Density Discrete Wavelet transform. *IEEE Transaction on Signal Processing, 54*(8): 3039-3048.
[56]. Jianwei Ma., & Gerlind Plonka, (2010). The Curvelet transform. *IEEE Signal Processing Magazine, 27*(2): 118-133.
[57]. Minh N. Do., and Martin Vetterli., (2005). The contourlet transform: An efficient directional multiresolution image representation. *IEEE Transaction on Image Processing*, *14*(12): 2091-2106.
[58]. Duncan D. Y. Po., and Minh N. Do., (2006). Directional multiscale modeling of images using the contourlet transform. *IEEE Transaction on Image Processing*, *15*(6): 1610-1620.
[59]. Wang-Q-Lim., (2010). The Discrete Shearlet transform: A new Directional Transform and compactly support shearlet Frames. *IEEE Transaction on Image Processing*, *19*(5): 1166-1180.
[60]. Jeena Roy., Salice Peter., and Neetha John., (2013). Denoising using Soft Thresholding. *International Journal of Advanced Research in Electrical, Electronics and Instrumentation Engineering.*
[61]. Wang, Z., Bovik, A.C., Sheikh, H.R., and Simonelli, E.P., (2004). Image quality assessment: From error measurement to structural Similarity. *IEEE Transactions on Image processing*, *13*(1): 600-612.
[62]. Zhou Wang., and Alan C Bovik., (2002). A Universal Image Quality Index. *IEEE Signal Processing Letters*.
[63]. Lin Zhang., Lei Zhang., Mou, X., and Zhang, D., (2011). FSIM: A Feature Similarity Index for Image Quality Assessment. *IEEE Transactions on Image Processing, 20*(8): 2378-2386.

How to cite this article: Sujithra, M.S. and Sugitha, N. (2020). Restoration of Compressed Image using Hard Thresholding Method. *International Journal on Emerging Technologies*, *11*(3): 975–982.